Theory of a lossless nonlinear Fabry-Perot interferometer

J. H. Marburger and F. S. Felber
University of Southern California, Los Angeles, California 90007
(Received 1 June 1976)

A Fabry-Perot interferometer filled with a medium whose refractive index depends upon intensity has a multiple-valued transmission-vs-intensity characteristic. When the incident light is circularly polarized, and the nonlinearity is only cubic in the fields, Maxwell's equations may be solved exactly for the plane-parallel resonator field in terms of elliptic functions. An accurate approximate analysis is given for more general cases, including resonators with spherical mirrors and finite beams, where self-focusing is important. The theory is developed to yield design information for operation as an optical switch, "transistor," and power limiter.

I. INTRODUCTION

The possibility of constructing a bistable optical device consisting of a multiple pass interferometer containing a saturable absorber was appreciated as early as 1969 by Seidel and by Szöke *et al.*[1] Experimental efforts to observe bistable operation prior to 1972 (reviewed in detail by Austin[2]) were frustrated primarily by the difficulty of maintaining adequate cavity finesse with an absorbing intracavity medium. This problem was overcome quite recently by Gibbs, McCall, and Venkatesan,[3] who found that bistable operation can also occur when the nondissipative (reactive) part of the cavity response is nonlinear. They succeeded in demonstrating bistability and other interesting modes of operation, and in constructing a theory which includes both reactive and dissipative nonlinearity, and adequately described their experimental results. At about the same time (but after Gibbs *et al.* had demonstrated their device) we developed a theory of bistable operation for purely reactive, nondissipative, nonlinear interferometers.[4] The absence of dissipation allows the theory to be carried quite far analytically, and in this paper we present a detailed description of the operation of the nondissipative nonlinear multiple pass interferometer. Our primary interest is in interferometers filled with media whose nonlinearity is not resonantly enhanced. In this case a variety of experimental arrangements are possible involving several incident beams of different frequencies.

The most tractable model for the nonlinear medium is one in which the susceptibility is regarded as a function of the time-averaged (over a few optical cycles) squared field. For circularly polarized fields the time average equals the nonaveraged squared field, and an exact treatment is possible for cubic nonlinearity and plane parallel reflectors with normal incidence (see Sec. II). An approximate theory, based on the slowly varying envelope approximation, is also possible, and leads to simpler expressions. This approximate theory, given in Sec. III for plane parallel reflectors, provides the starting point for a discussion of nonplanar (e.g., confocal) reflectors and finite beams contained in Sec. IV. Using a variational method[5] which leads to equations in another context which have been shown to be valid for powers somewhat below the critical power for self-focusing,[6] we can rather simply include the effects of self-focusing on the nonlinear interferometer operating parameters.

In Sec. V, we develop the exact solutions of the slowly varying envelope equations for the case treated approximately in Sec. IV. These solutions, briefly discussed previously by Glass[7] and Suydam,[8] are the nonlinear generalization of the self-similar modes of a cavity with spherical resonators. For plane mirrors, they reduce to the self-trapped modes of which the lowest-order case was first discussed by Chiao, Garmire, and Townes.[9] After a slight renormalization, the resonance condition predicted by the variational approach agrees so closely with the numerical result that cavity design calculations can be based with confidence on the analytically tractable results of Sec. IV.

In Sec. VI we indicate design parameters for several practical cases. Switching powers as low as 35 W are possible with CS_2 in a cavity with 90% reflectors, and in two-frequency operation (switching field tuned to a cavity resonance) even lower switching powers are possible. Use of high-n_2 materials such as the nematic liquid crystal MBBA reduces the required powers below 1W.

II. EXACT THEORY FOR PLANE-PARALLEL REFLECTORS

If the optical field depends only upon the coordinate z along the length of the cavity, and upon time t, then within the cavity the field is transverse and obeys

$$c^2\partial_z^2 \vec{E} = \partial_t^2 (\vec{E} + 4\pi\vec{P}) \quad \text{(Gaussian units)} . \tag{1}$$

If the incident beam is monochromatic with angular frequency ω, and if the nonlinear part of the polarization density $\vec{P}$ contributes neither loss nor new frequencies, then (1) becomes

$$\vec{E}'' = -\vec{E} - 4\pi\vec{P} , \tag{2}$$

where primes denote differentiation with respect to $\zeta \equiv \omega z/c$. This ordinary differential equation for $\vec{E}(\zeta)$ may be integrated in closed form for many special cases. Let us suppose, for example, that the envelopes of $\vec{P}$ and $\vec{E}$ defined through

$$\vec{P} = \mathrm{Re}\vec{\mathcal{P}} e^{-i\omega t}, \quad \vec{E} = \mathrm{Re}\vec{\mathcal{E}}\, e^{-i\omega t}$$

satisfy

$$\mathcal{P}_i = \chi^{(1)}(\omega)\mathcal{E}_i + 3\chi^{(3)}_{ijkl}(\omega; -\omega, \omega, \omega)\mathcal{E}_j^* \mathcal{E}_k \mathcal{E}_l \tag{3}$$

in the notation of Maker and Terhune.[10] If the nonlinear medium is isotropic, then $\vec{\mathcal{P}}$ may be written

$$\vec{\mathcal{P}} = (n_0^2 - 1)\vec{\mathcal{E}} + \eta |\vec{\mathcal{E}}|^2 \vec{\mathcal{E}} \tag{4}$$

when the field is either linearly or circularly polarized. For linear polarization

$$\eta_1 = 3\chi^{(3)}_{1111} = 3(\chi^{(3)}_{1122} + \chi^{(3)}_{1212} + \chi^{(3)}_{1221}) , \tag{5}$$

and for circular polarization

$$\eta_c = 3(\chi^{(3)}_{1212} + \chi^{(3)}_{1221}) . \tag{6}$$

Let us continue with circularly polarized fields. In this case $\vec{E}^2 = \frac{1}{2}|\vec{\mathcal{E}}|^2$, and (2) with (3) leads to

$$\vec{E}'' = -n_0^2\vec{E} - 8\pi\eta_c E^2\vec{E} . \tag{7}$$

This equation is equivalent to that describing the motion of a particle of unit mass in two dimensions in the conservative potential

$$V = \tfrac{1}{2} n_0^2 E^2 + 2\pi\eta_c E^4 , \tag{8}$$

where $\vec{E}$ is the "position" vector and ζ the "time." The corresponding Lagrangian is

$$L = \tfrac{1}{2}\vec{E}'^2 - V(E)$$
$$= \tfrac{1}{2}E'^2 + \tfrac{1}{2}E^2\theta'^2 - V(E) , \tag{9}$$

where on the second line $\theta = \tan^{-1}(E_y/E_x)$, and of course E is the magnitude of $\vec{E}$. Since θ does not appear in the Lagrangian, the canonically conjugate "angular momentum" $S \equiv -\partial L/\partial\theta'$ is a constant of the motion:

$$S = -E^2\theta' = -E_x E_y' + E_y E_x' = \hat{z}\cdot\vec{E}\times\vec{B} . \tag{10}$$

The last line follows from Maxwell's equations and the fact that the fields are circularly polarized. S differs from the usual canonical momentum by a minus sign to emphasize its relation to the Poynting vector.

Using the conserved energy

$$H = \tfrac{1}{2}E'^2 + \tfrac{1}{2}(S^2/E^2) + V(E) , \tag{11}$$

one finds $E(\zeta)$ from the usual energy integral

$$\zeta - \zeta_0 = \int_{E_0}^{E} \frac{dE}{[2H - (S^2/E^2) - 2V(E)]^{1/2}}$$
$$= \int_{I_0}^{I} \frac{dI}{[2HI - 2V(I)I - S^2]^{1/2}} , \tag{12}$$

where $I \equiv E^2$. When V has the form of Eq. (8), (12) is an elliptic integral of the first kind. Taking ζ_0 at the position ζ_+ of a maximum where $I = I_+$, one finds

$$I = I_- + (I_+ - I_-)\, \mathrm{cn}^2\, \nu(\zeta - \zeta_+) , \tag{13}$$

where cn is a Jacobian elliptic function, and I varies between I_- and I_+ in the nonlinear medium. The parameter ν, which plays the role of a refractive index, is defined by

$$\nu^2 = n_0^2 + 4\pi\eta_c (I_- + 2I_+) . \tag{14}$$

The parameter m of the elliptic function is

$$m = 4\pi\eta_c (I_+ - I_-)/\nu^2 . \tag{15}$$

If the total field $\vec{E}$ is resolved into forward and backward travelling components according to

$$\vec{E} = \vec{E}_F + \vec{E}_B, \quad \vec{E}_{F,B} = \mathrm{Re}\hat{u}_R \mathcal{E}_{F,B} e^{-i\omega t} ,$$

then defining $E_F = (\vec{E}_F \cdot \vec{E}_F)^{1/2}$, etc., we find

$$E^2 = E_F^2 + E_B^2 + 2E_F E_B \cos(\phi_F - \phi_B) , \tag{16}$$

where $\phi_{F,B}$ is the phase of $\mathcal{E}_{F,B}$, and $\hat{u}_R$ is the unit right-circular polarization vector. Recall that the sense of rotation of circular polarization is not altered on reflection (the helicity changes sign on reflection). Comparison of (16) with (13) gives immediately

$$I_\pm = (E_F \pm E_B)^2, \tag{17}$$

$$\cos\tfrac{1}{2}(\phi_F - \phi_B) = \mathrm{cn}\nu(\zeta - \zeta_+) . \tag{18}$$

Thus the amplitude of the elliptic function is half the phase difference between the forward and backward travelling fields.

To find the transmissivity $\mathcal{T}$ of an interferometer with mirrors of reflectance R located at $z = 0$ and $z = D$, we first remark that at the back mirror (at D) the phases of forward and backward travelling fields must coincide (assuming $n_0 > 1$ and vacuum outside the cavity). Thus

$$\mathrm{cn}\nu(\zeta_D - \zeta_+) = 1. \tag{19}$$

and $\zeta_+ = \zeta_D \equiv \omega D/c$. Also at the back mirror, flux conservation requires

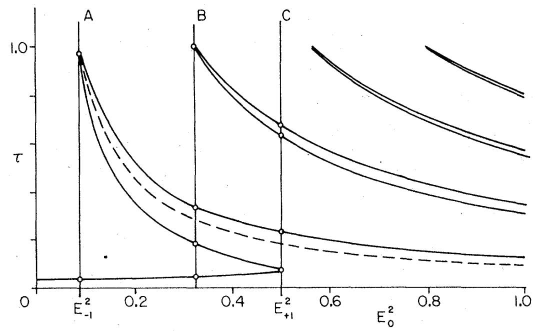

FIG. 1. Transmissivity τ vs dimensionless input intensity $I_0=E_0^2$ for a plane nonlinear interferometer with mirror reflectivity $R=70\%$ and detuning angle $\delta=-\frac{3}{4}\pi$. $E_\pm$ are "on" and "off" fields for single-frequency bistable operation.

$$(1-R)n_0E_F^2=I_T\,, \tag{20}$$

$$E_B^2=RE_F^2=RI_T/(1-R)n_0\,, \tag{21}$$

$$I_T=S\,, \tag{22}$$

where I_T is the transmitted intensity. These equations fix E_F and E_B and therefore also $I_\pm$, as functions of the net flux S.

At the front mirror ($\zeta=0$), the condition that the forward field equals the transmitted part of the incident field plus the reflected part of the backward field leads to

$$(1-R)I_0/n_0=E_F^2+RE_B^2-2R^{1/2}E_FE_B\cos(\phi_F-\phi_B)$$

or, using (20)–(22) and (18), to

$$I_0=[S/(1-R)^2]\,[(1+R)^2-4R\,\mathrm{cn}^2(\nu\zeta_D)]\,, \tag{23}$$

where $I_0=E_0^2$ is the intensity incident on the interferometer. Since ν and the parameter m of cn are fixed by $I_\pm$, and hence by S, Eq. (23) fixes I_0 in terms of S. But the transmissivity is defined by

$$\mathcal{T}=I_T/I_0=S/I_0\,. \tag{24}$$

Therefore $\mathcal{T}$ is determined as a function of I_0 by the parametric equations (23) and (24), with parameter S. Equation (24) may be rewritten as

$$\mathcal{T}=(1+F\,\mathrm{sn}^2\nu\zeta_D)^{-1}\,, \tag{25}$$

where $F=4R/(1-R)^2$. This is identical in form to the usual formula for the transmission of a Fabry-Perot interferometer[11] except that $\mathrm{sn}\nu\zeta_D$ replaces $\sin n_0\zeta_D$.

The striking feature of Eq. (25) is of course that $\mathcal{T}$ depends upon the incident intensity. Moreover, it is multiple valued as shown in Fig. 1. The transmission peaks occur when $\nu\zeta_D$ is a multiple of the half period $2K(m)$ or twice the complete elliptic integral of the first kind. Further discussion of the properties of the nonlinear interferometer are much more convenient in the context of an approximate theory in which the nonlinear index change is small compared with n_0.

III. APPROXIMATE THEORY FOR PLANE-PARALLEL REFLECTORS

If in Eq. (7) we introduce the notation

$$\vec{\mathrm{E}}=\mathrm{Re}(\vec{\mathcal{E}}_F e^{ikz}+\vec{\mathcal{E}}_B e^{-ikz})e^{i\omega t}\,, \tag{26}$$

we can derive equations for the envelope functions $\vec{\mathcal{E}}_F$ and $\vec{\mathcal{E}}_B$. (This notation differs from that in Sec. II where $\mathcal{E}$ includes rapid z-dependence.) When the fields are not too strong, we expect nearly all the rapid spatial dependence to be included in the phase $kz=n_0\zeta$, and therefore the slowly varying envelope approximation should be valid (ignore $|\mathcal{E}_F''/k\mathcal{E}_F'|$, etc.) The equation for $\mathcal{E}_F$ may be found by multiplying the positive frequency part of (7) by e^{-ikz} and averaging over a few spatial periods. Our results will be valid for both linear and circular polarization if E^2 in (7) is replaced by its time average. The resulting equations are

$$2ik\partial_z\vec{\mathcal{E}}_F=-(4\pi\omega^2\eta/c^2)(|\mathcal{E}_F|^2+2|\mathcal{E}_B|^2)\vec{\mathcal{E}}_F\,, \tag{27}$$

$$-2ik\partial_z\vec{\mathcal{E}}_B=-(4\pi\omega^2\eta/c^2)(|\mathcal{E}_B|^2+2|\mathcal{E}_F|^2)\vec{\mathcal{E}}_B, \tag{28}$$

where $k=n_0\omega/c$, and the time-averaged intensity E^2 is $\frac{1}{2}|\mathcal{E}|^2$. It is easy to show from these equations that $|\mathcal{E}_F|^2$ and $|\mathcal{E}_B|^2$ do not change with z, and that the phase difference is

$$\tfrac{1}{2}(\phi_F-\phi_B)=n_0\zeta+(3\pi\eta\zeta/n_0)(|\mathcal{E}_F|^2+|\mathcal{E}_B|^2)-\phi_0$$
$$=n_0\zeta+(3\pi\eta\zeta/n_0)(I_++I_-)-\phi_0\,. \tag{29}$$

In the limit of small η, this reduces to the phase implied by the exact result (18). The constant phase ϕ_0 is chosen to make $\phi_F=\phi_B$ at $\zeta=\zeta_D$, and may be written

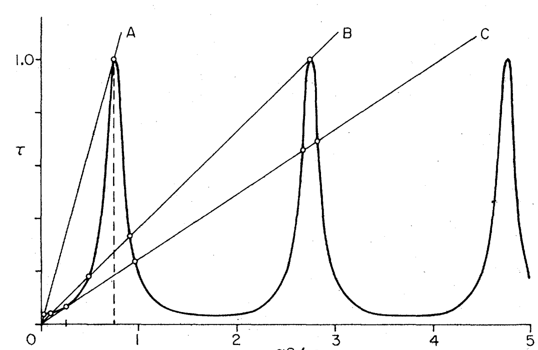

FIG. 2. Graphical determination of the τ-vs-I_0 curve of Fig. 1. The lines A, B, C and the dashed curve correspond to similarly labelled lines in Fig. 1. $R=70\%$, $\sigma=-\frac{3}{4}\pi$.

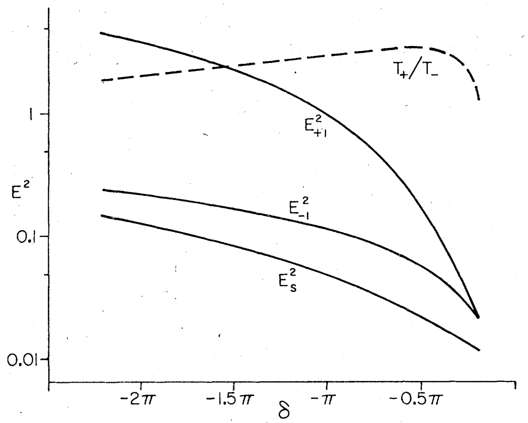

FIG. 3. "On" and "off" fields for bistable operation vs cavity detuning for $R=70\%$. E_s is the minimum switching field for two-frequency bistable operation. T_+/T_- is the ratio of "on" to "off" transmissivities at the "on" field.

$$\phi_0=\delta+\alpha S\ , \tag{30}$$

where $\alpha=6\pi\eta\zeta_D(1+R)/n_0^2(1-R)$, and $\delta=n_0\zeta_D$. Repeating the argument of Sec. II, we arrive at an expression for the transmissivity

$$\alpha S/\alpha I_0=\mathcal{T}(\delta+\alpha S)=[1+F\sin^2(\delta+\alpha S)]^{-1}\ . \tag{31}$$

In Fig. 2 we have plotted the right-hand side of (31) vs αS. If the incident intensity I_0 is specified, then the corresponding transmissivity may be found from the intersection of a straight line of slope $1/\alpha I_0$ with the $\mathcal{T}$-vs-αS curve. This construction, shown in Fig. 1, clearly illustrates the multiple-valued nature of $\mathcal{T}$-vs-I_0 curve: for sufficiently large I_0, there are several intersections. For practical values of the nonlinear index change, Eq. (31) leads to results indistinguishable from the exact solution (23) and (24).

Figure 3 summarizes the dependence of the characteristic features of the transmissivity curve on the detuning parameter δ. Of particular interest are the minimum "holding" intensity I_{-1} required to maintain $\mathcal{T}$ near unity in the first "on" branch of the $\mathcal{T}$-vs-I_0 curve, and the "turn-on" intensity I_{+1} required to pass from the "off" to the first "on" branch. Since the nonlinear response is in general nonresonant, one may reduce the turn-on intensity by tuning the frequency of the switching field into resonance with the cavity. If the net flux S_+ is required to switch the cavity on for the signal field at frequency ω, then (31) gives the least required incident switching intensity $I_s=S_+$ at the detuned frequency ω'. Here ω' is chosen to make $\mathcal{T}=1$. Figure 3 shows that the detuned switching field is less than the holding signal over the entire detuning range. Thus a strong signal at ω may be switched by a somewhat weaker signal at ω'. The required detuning $\omega-\omega'$ is clearly always less than the cavity mode spacing. Numerical examples will be deferred to Sec. VI, after the finite beam theory is developed.

IV. APPROXIMATE THEORY FOR RESONATOR WITH SPHERICAL MIRRORS

When the field amplitudes depend upon the transverse variables (x, y), then Eqs. (27) and (28) have the additional terms $\nabla_T^2\vec{\mathcal{E}}_F$ and $\nabla_T^2\vec{\mathcal{E}}_B$, respectively, on the left-hand side, where $\nabla_T^2=\partial_x^2+\partial_y^2$. The resulting equations describe self-focusing in a resonator, and it is necessary to determine under what conditions the interferometer can be operated without incurring a catastrophic self-focus within the cavity. We shall employ an approximate analysis based upon a variational method used by Vorob'yev for elliptical beam self-focusing.[5]

Equations (27) and (28), with the ∇_T^2 terms, may be derived from the Lagrangian density

$$\begin{aligned}\mathcal{L}=&|\nabla_T\mathcal{E}_F|^2+|\nabla_T\mathcal{E}_B|^2-ik(\mathcal{E}_F^*\partial_z\mathcal{E}_F-\mathcal{E}_F\partial_z\mathcal{E}_F^*)\\&+ik(\mathcal{E}_B^*\partial_z\mathcal{E}_B-\mathcal{E}_B\partial_z\mathcal{E}_B^*)\\&-(2\pi\omega^2\eta/c^2)(|\mathcal{E}_F|^4+|\mathcal{E}_B|^4+4|\mathcal{E}_F\mathcal{E}_B|^2)\end{aligned} \tag{32}$$

and the variational principle

$$\delta\int L\,dz=\delta\int\left(\int dx\int dy\,\mathcal{L}\right)dz=0\ . \tag{33}$$

Our approximation consists in evaluating (33) using the trial functions

$$\begin{aligned}\mathcal{E}_F&=\frac{\mathcal{E}_{F0}a_0}{a}\exp\left[-\left(\frac{r^2}{2a^2}-i\frac{kr^2a'}{2a}+i\psi_F\right)\right],\\ \mathcal{E}_B&=\frac{\mathcal{E}_{B0}b_0}{b}\exp\left[-\left(\frac{r^2}{2b^2}+i\frac{kr^2b'}{2b}+i\psi_B\right)\right],\end{aligned} \tag{34}$$

where $\mathcal{E}_{F0}$, $\mathcal{E}_{B0}$, ψ_F, ψ_B, a and b are functions of z chosen to satisfy (33), and $r^2=x^2+y^2$. Primes denote differentiation with respect to z. The quantities $\mathcal{E}_{F0}$ and $\mathcal{E}_{B0}$ are found to be constant and are related to the conserved forward and backward powers

$$P_F=\tfrac{1}{8}n_0ca_0^2|\mathcal{E}_{F0}|^2,\quad P_B=\tfrac{1}{8}n_0cb_0^2|\mathcal{E}_{B0}|^2\ . \tag{35}$$

Upon substituting (34) into (32) and (33), integrating over the transverse plane, and writing out the Euler-Lagrange equations implied by (33), one finds equations for a, b, ψ_F, and ψ_b which can be integrated simply in some special cases. Here we are interested only in the high finesse case where $P_F\approx P_B$, and the forward and backward beam radii are essentially equal on any plane of constant z. When $P_F\neq P_B$, the forward and backward beams have waists which do not coincide. When $P_F=P_B=P$, solutions exist for which $a(z)=b(z)$, and the Euler

Lagrange equation for a becomes

$$k^2a'' = (1 - 3P/P_c)/a^3 \; . \qquad (36)$$

Here $P_c = n_0c^3/8\pi\eta\omega^2$ is the critical power for self-trapping (self-focusing just balances diffraction) in this theory for a purely forward travelling beam. It is four times greater than the critical power P_1 predicted by the "aberrationless"[12] approximation and very close to the correct value $P_2 = 3.77P_1$ inferred from numerical solutions.[6] According to (36), the critical power for formation of a singular self-focus at the beam waist is reduced by a factor of $\frac{1}{3}$ in a cavity with 100% reflectors. Taking the origin of z at the point where the rays are parallel to the z axis, we may write the solution $a(z)$ of (36) as

$$a^2(z)/a_0^2 = 1 + (1 - 3P/P_c)(z/ka_0^2)^2 \; , \qquad (37)$$

where $a_0 = a(0)$. This result may be used in the Euler-Lagrange equation for the axial phase ψ

$$-2k\psi_F' = (2 - 9P/P_c)/a^2 \qquad (38)$$

to obtain

$$\psi_F(z) = -\frac{1 - 9P/2P_c}{(1 - 3P/P_c)^{1/2}} \times \tan^{-1}\left[\left(1 - \frac{3P}{P_c}\right)^{1/2} \frac{z}{ka_0^2}\right] + \psi_{F0}. \qquad (39)$$

The backward phase looks the same, but with the sign of the first term reversed.

Let us use this result to analyze the nonlinear behavior of the family of symmetric stable resonators whose mirrors coincide with surfaces of constant phase of our Gaussian trial functions (34). Equation (37) is identical to the spot size formula for linear Gaussian propagation if k^2 is increased by the factor $(1 - 3P/P_c)^{-1}$. Consequently, most of the equations describing the nonlinear resonator resemble closely those familiar from the linear theory.[13] In particular, the waist radius a_0 for mirror spacing D and radius of curvature R_c is fixed by

$$(ka_0^2)^2 = \tfrac{1}{4}(1 - 3P/P_c)D(2R_c - D) \rightarrow \tfrac{1}{4}(1 - 3P/P_c)D^2 \quad (R_c = D) \; , \qquad (40)$$

where the last line is correct for a confocal cavity. The spot size a_1 at the mirrors satisfies

$$(ka_1^2)^2 = (1 - 3P/P_c)R_c^2D/(2R_c - D) \rightarrow (1 - 3P/P_c)D^2 \quad (R_c = D).$$

The nonlinear phase difference $\frac{1}{2}(\psi_F - \psi_B)$ which we require for our transmissivity analysis is given by (39) and (40):

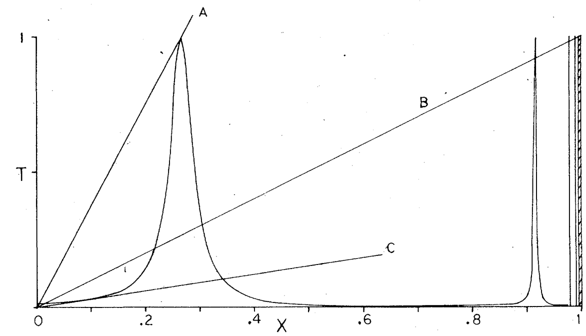

FIG. 4. Graphical determination of τ vs νP_0 for confocal nonlinear interferometer with mirror reflectivity $R = 90\%$. See Eq. (43). Compare with Fig. 2. Only the first two cavity resonances and the center lines of the third and fourth are drawn. Beyond the fifth the resonances are too closely spaced to distinguish.

$$\tfrac{1}{2}(\psi_F - \psi_B) = \Delta - \frac{1 - 9P/2P_c}{(1 - 3P/P_c)^{1/2}} \times \tan^{-1}\left(\frac{2z}{[D(2R_c - D)]^{1/2}}\right). \qquad (41)$$

As before we choose Δ so the total phase difference vanishes at the exit mirror at $z = \frac{1}{2}D$. Thus at the entrance mirror ($z = -\frac{1}{2}D$), (41) gives

$$\tfrac{1}{2}(\psi_F - \psi_B) = -kD + 2\frac{1 - 9P/2P_c}{(1 - 3P/P_c)^{1/2}} \tan^{-1}\left(\frac{D}{2R_c - D}\right)^{1/2} \rightarrow -kD + \tfrac{1}{2}\pi\frac{1 - 9P/2P_c}{(1 - 3P/P_c)^{1/2}} \quad (R_c = D) \; . \qquad (42)$$

The phase (42) is all we need to derive a parametric equation for the transmissivity versus the incident power P_0 similar to Eqs. (23), (24), or (31). By analogy with (29), we can hope to correct our error in setting $P_F = P_B = P$ by replacing P by

$$P = \tfrac{1}{2}(P_F + P_B) = P_s(1 + R)/2(1 - R) \; ,$$

where P_s is the net energy flux through the medium. The implicit equation for P_s, corresponding to (31), is

$$\nu P_s/\nu P_0 = \mathcal{T}(\nu P_s) = \{1 + F\sin^2[\delta + f(\nu P_s)]\}^{-1} \; , \qquad (43)$$

where F and δ are the same as in (31), and

$$f(x) \equiv -\frac{2 - 3x}{(1 - x)^{1/2}}\tan^{-1}\left(\frac{D}{2R_c - D}\right)^{1/2} \rightarrow -\tfrac{1}{4}\pi(2 - 3x)/(1 - x)^{1/2} \quad (R_c = D); \qquad (44)$$

$$\nu \equiv 3(1 + R)/2(1 - R)P_c \, .$$

Equation (43) may still be solved graphically as in Fig. 2, but the right-hand side is no longer identi-

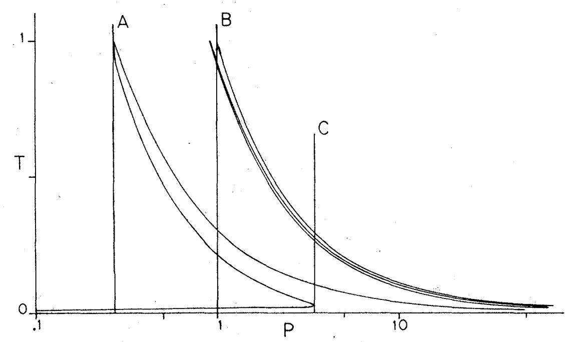

FIG. 5. Transmissivity τ vs νP_0 determined by construction of Fig. 4. Compare with Fig. 1. We show only the first two resonances and the limiting curve (corresponding to formation of a catastrophic self-focus in the cavity). Units of P are $1/\nu$.

cal to the linear Fabry-Perot tuning curve because $f(\nu P_s)$ is not linear (see Fig. 4).

The singular denominator of (44) ensures that an infinite nonlinear tuning range is possible for powers below the critical power for catastrophic

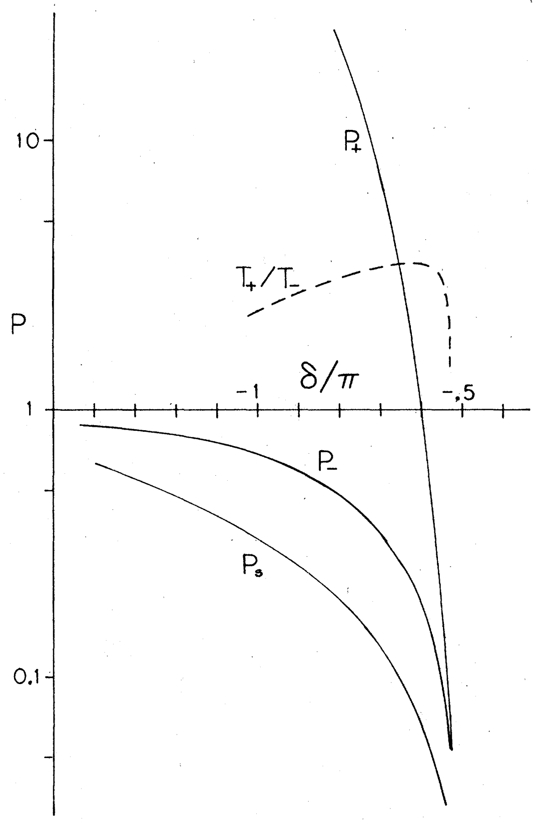

FIG. 6. "On" and "off" powers for single- and double-frequency operation of a confocal cavity. Compare with Fig. 3. Power units are $1/\nu$.

self-focus formation at $\frac{1}{3}P_c$. Figures 4 and 5 show how the infinity of Fabry-Perot resonances are squeezed into the range $0 \leq \nu P_s \leq 1$. The graphical solution shows that the incident power required to hold the interferometer in the "on" state can never exceed $1/\nu \approx \frac{1}{3}(1-R)P_c$ for high mirror reflectivity. The power at frequency ω_1 required to turn the cavity transmissivity "on" for a signal at ω, when ω_1 is tuned to minimize this power, is also less than $1/\nu$. Figure 6 shows curves for turn-on and holding powers for a confocal cavity.

It is unfortunately not possible to reduce the solutions in this section to those of Secs. I–III for beams infinite in transverse extent. The problem is that the phase of a finite beam includes an additional nonlinear contribution because it is partially confined by a self-induced waveguide. This effect decreases the phase velocity below the value expected from the direct nonlinear index change.

V. EXACT SOLUTIONS OF SVEA EQUATIONS FOR A RESONATOR WITH SPHERICAL MIRRORS

If, as in Sec. IV, we assume that at each point within the cavity the net flux vanishes, then $|\mathcal{E}_F|^2 = |\mathcal{E}_B|^2$, and Eq. (27) becomes

$$2ik\partial_z \mathcal{E}_F + \nabla_T^2 \mathcal{E}_F = -(4\pi\omega^2\eta/c^2)3\,|\mathcal{E}_F|^2\mathcal{E}_F\,. \tag{45}$$

This has the same form as the slowly varying envelope equation for a self-focusing beam travelling to the right, except that η is increased by the factor 3. The self-focusing equation is known to possess similarity solutions of the form[6-8]

$$\mathcal{E}_F = a^{-1} f(r/a) e^{iS_F}\,,$$

where a^2 is a quadratic function of z. If the origin of z is chosen where $da/dz = a' = 0$, then

$$a^2(z)/a_0^2 = 1 + (\beta z/k a_0^2)^2\,. \tag{47}$$

The phase required for self-similarity is

$$S_F = -(\alpha/2\beta)\tan^{-1}(\beta z/k a_0^2) - k r^2 a'/2a\,, \tag{48}$$

where

$$\alpha = -2 + (12\pi\omega^2\eta/c^2) f^2(0)\,, \tag{49}$$

and f satisfies

$$f'' + f'/\rho = (\alpha + \beta^2\rho^2) f - (12\pi\omega^2\eta/c^2) f^3\,, \tag{50}$$

in which a prime denotes a derivative with respect to $\rho = r/a$. The parameter β is related to the incident power and the axial field $f(0)$. In practice one fixes β and determines $f(0)$ such that the solution of (50) has no nodes (for the analog of the TEM_{00} mode) and decays to zero at large radial distances. When $\beta = 0$, the nodeless solution reduces to the Chiao, Garmire, and Townes self-trapped mode.[9]

Equation (47) is, as (37), identical to the spot size formula for linear Gaussian propagation if k is simply increased by the factor $1/\beta$. Thus β^2 in (47) plays the role of $1-3P/P_c$ in (37). The spot size formulas for a symmetric cavity with spherical mirrors are similar to (40) and (41):

$$(ka_0^2)^2 = \tfrac{1}{4}\beta^2 D(2R_c - D)\ , \tag{51}$$

$$(ka_1^2)^2 = \beta^2 R_c^2 D/(2R_c - D). \tag{52}$$

The phase difference at the entrance mirror corresponding to (42) is

$$\tfrac{1}{2}(\phi_F - \phi_B) = -kD - (\alpha/\beta)\tan^{-1}[D/(2R_c - D]^{1/2}. \tag{53}$$

To find the ratio α/β numerically, it is convenient to cast (50) into dimensionless form. Setting $x^2 \equiv |\alpha|\rho^2$, and $y^2 \equiv 12\pi\omega^2\eta f^2/c^2|\alpha|$, one finds

$$y'' + y'/x = y\,\mathrm{sgn}\,\alpha + (\beta^2/\alpha^2)x^2 y - y^3 \tag{54}$$

and

$$\alpha = \pm 2/(y_0^2 \mp 1)\ ,$$

where the upper (lower) sign is for $\alpha > 0$ ($\alpha < 0$). If the dimensionless power p is defined as

$$p = \int_0^\infty x\,dx\,y^2\ , \tag{55}$$

then the actual power is easily seen to be

$$P = \tfrac{1}{6}pP_c\ . \tag{56}$$

Figure 7 shows $\alpha/2\beta$ and β^2 vs $3P/P_c$ computed from (54). On the same graph is drawn the approximate expressions derived in Sec. IV. The approximate phase (42) which is the only parameter required for our interferometer theory, agrees almost exactly with the "exact" self-similar phase expression if P_c is replaced by the actual critical power $1.07P_c$. The much poorer agreement between β^2 and $1-3P/P_c$ can perhaps be understood as a consequence of the significant departure of the shape $f(\rho)$ from the Gaussian function assumed in the approximate theory.

FIG. 7. Comparison of exact numerical solutions for the axial phase factor for the self-similar modes of a nonlinear confocal cavity (circles) and the phase predicted by the variational approximation (solid curve). The dashed curve is the renormalized approximate theory. Also shown is the spot size factor β^2 (crosses) and the unrenormalized approximate result $1 - 3P/P_c$ (solid line).

In view of the very widespread use of the aberrationless approximation in self-focusing theory,[12] we should point out that that approximation does not give results for the phase in agreement with the exact SVEA self-similar solutions. The aberrationless equations are derived by substituting the Gaussian trial functions (34) into the SVEA equations and matching coefficients of r^{2n} for $n = 0, 1$. The resulting equations analogous to (36) and (38) are

$$k^2 a'' = (1 - 3P/P_1)/a^3\ , \tag{57}$$

$$-2k\psi_F' = (2 - 3P/P_1)/a^2\ , \tag{58}$$

where $P_1 = \frac{1}{4}P_c$. Even if P_1 is replaced by the correct critical power, the phase is poorly represented by (58).

VI. DISCUSSION AND NUMERICAL EXAMPLES

The tuning curves of Fig. 6 show that even for a cavity with the modest finesse of 30, powers on the order of $1/10\nu$ suffice to change a confocal nonlinear interferometer from a reflecting to a transmitting state. Taking $\eta = n_0 n_2/4\pi$, and replacing P_c by $P_c/0.93$, we can write $1/\nu$ as

$$1/\nu = 27.2(\lambda^2/n_2)(1-R)/(1+R) \quad \text{Watts}\ ,$$

where λ is in cm and n_2 in esu. Thus for CS_2 ($n_2 \approx 10^{-11}$ esu for linear polarization), $\lambda = 500$ nm, and $R = 90\%$, we have $1/\nu = 357$ W, so that operating powers on the order of 35 W are possible. Materials with much greater nonlinear indices are available. The nematic liquid crystal MBBA, for example, has a nonlinearity about 70 times larger than that of CS_2.[14] Using 90% reflectors one should therefore be able to observe bistable operation with switching powers on the order of 0.5 W. Even smaller powers could be used with higher finesse, longer cavities, and multiple-frequency operation (switching with frequency ω_1 and holding with frequency ω).

If the detuning angle is small, the transmissivity of the nonlinear interferometer is a sensitive function of the incident intensity, and may be operated in a "transistor" mode similar to that demonstrated by Gibbs *et al.*[3] In this mode one biases the incident field with a cw beam which tunes the cavity nonlinearly to a region where the $\mathcal{T}$-vs-P_0 curve is nearly vertical. Then a small modulation on the bias beam causes large changes in the transmissivity, with consequent large modulated output signal. The transfer curve for such operation is obtained by multiplying the $\mathcal{T}$-vs-P_0 curve by P_0. In another interesting mode of operation, the transmissivity at frequency ω can be modulated by a relatively weak signal at ω_1, where the cavity is just off resonance for ω but resonant for ω_1. In still another mode the device operates as a power stabilizer since, as can be seen from the graphical solution for $\mathcal{T}$ vs P_0 (Fig. 5), the transmissivity is nearly inversely proportional to the incident power on the "on" branch of the operating curve.

In all of these applications, the response time of the device is limited either by the response time of the cavity, which is roughly

$$\tau_{\text{cav}} \simeq 2n_0 D/c\,|\ln R|\ ,$$

or by the response time τ of the nonlinearity. For a 1-cm cavity with 90% reflectors, τ_{cav} is about 1 nsec. The medium response time is sensitive to the nature of the nonlinear mechanism. In CS_2, where molecular reorientation is dominant, τ is about 2 psec. In the liquid crystal MBBA, $\tau \simeq 40$ nsec.[14] New solid materials are being developed which have nonlinearities comparable to MBBA, but with response times many orders of magnitude shorter.[15] The possibility of very short switching times is one of the significant advantages of nonresonant operation.

VII. SUMMARY

We have shown that exact analytical solutions may be obtained in parametric form for the transmissivity of a nonlinear plane-parallel Fabry-Perot interferometer with cubic nonlinearity and circular polarization. At low intensities the equations in the slowly varying envelope approximation (SVEA) which can also be solved exactly for this case, give results in excellent agreement with the exact solutions. This agreement lends credibility to the SVEA predictions for interferometers with spherical mirrors. We could obtain tractable equations in this case only in the limit that forward and backward powers were equal (high finesse case), whereupon the cavity modes are identical to the self-similar modes of self-focusing beams. Using a variational method, we found analytical expressions for the phases of the forward and backward amplitudes which again allowed the transmissivity to be expressed analytically in parametric form. The phases obtained this way agree almost identically with the numerical solutions of the SVEA self-focusing equations after the critical power is renormalized. Thus simple, reliable expressions are available for the transmissivity of a nonlinear interferometer with spherical mirrors. Because of the effective index change associated with self-induced waveguiding in the spherical mirror geometry, the powers required for bistable operation are reduced substantially relative to the plane mirror geometry.

[1]H. Seidel, U. S. Patent No. 3 610 731 (1969); A. Szöke, V. Daneu, J. Goldhar, and N. A. Kurnit, Appl. Phys. Lett. 15, 376 (1969).

[2]J. W. Austin, Ph.D. dissertation (University of Southern California, 1972) (unpublished).

[3]S.L. McCall, H. M. Gibbs, and T. N. C. Venkatesan, J. Opt. Soc. Am. 65, 1184 (1975); S. L. McCall, H. M. Gibbs, G. G. Churchill, and T. N. C. Venkatesan, Bull. Am. Phys. Soc., April, 1975, 636; H. M. Gibbs, S. L. McCall, and T. N. C. Venkatesan, Phys. Rev. Lett. 36, 1135 (1976).

[4]F. S. Felber and J. H. Marburger, Appl. Phys. Lett. 28, 731 (1976). (In this paper, we remarked that "the origin of the multistable operation described here is quite different from that studied previously." It is clear, however, from Ref. 3 above that Gibbs *et al.* were indeed aware of the importance of the reactive component of the nonlinear response in the operation of their device, and had included it in their theory.)

[5]V. V. Vorob'yev, IVUZ Radiofiz. 12, 1905 (1970).

[6]J. H. Marburger, Prog. Quantum Electron. 4, 35 (1975).

[7]A. J. Glass (private communication).

[8]B. R. Suydam, Los Alamos Scientific Laboratory Report No. LA-5003-MS (1973) (unpublished).

[9]R. Y. Chiao, E. Garmire, and C. H. Townes, Phys. Rev. Lett. 13, 479 (1964); 14, 1056 (1965).

[10]P. D. Maker and R. W. Terhune, Phys. Rev. 137, A801 (1965).

[11]M. Born and E. Wolf, *Principles of Optics*, 4th ed. (Pergamon, New York, 1970).

[12]S. A. Akhmanov, R. V. Khokhlov, and A. P. Sukhovukov, Chap. E3 in *Laser Handbook*, edited by F. T. Avecchi and E. O. Schulz-DuBois (North-Holland, Amsterdam, 1972), Chap. E3; W. G. Wagner, H. A. Haus, and J. H. Marburger, Phys. Rev. 175, 256 (1968).

[13]A. Yariv, *Introduction to Optical Electronics*, Holt, Rinehart and Winston, New York, 1971).

[14]G. K. L. Wong and Y. R. Shen, Phys. Rev. Lett. 30, 895 (1973).

[15]C. Sauteret, J. P. Herman, R. Frey, E. Pradere, J. Ducuing, R. H. Baugham, and R. R. Chance, Opt. Commun. 18, 55 (1976).